Journal of Hazardous Materials 168 (2009) 507–514

Contents lists available at ScienceDirect

Journal of Hazardous Materials

journal homepage: www.elsevier.com/locate/jhazmat

Optimal exponential feeding strategy for dual-substrate biostimulation of phenol degradation using *Cupriavidus taiwanensis*

Bor-Yann Chen [a], Jun-Wei You [b], Jo-Shu Chang [b,c,*]

[a] Department of Chemical and Materials Engineering, National I-Lan University, I-Lan 260, Taiwan
[b] Department of Chemical Engineering, National Cheng-Kung University, Tainan 701, Taiwan
[c] Sustainable Environment Research Center, National Cheng Kung University, Tainan 701, Taiwan

ARTICLE INFO

Article history:
Received 30 November 2008
Received in revised form 11 February 2009
Accepted 11 February 2009
Available online 21 February 2009

Keywords:
Cupriavidus taiwanensis
Dual substrate
Exponential feeding
Fed-batch culture
Phenol biodegradation

ABSTRACT

The exponential feeding strategy (EFS) of dual substrates (i.e., phenol and glycerol) was applied to optimize the overall performance of phenol degradation by *Cupriavidus taiwanensis* R186. Addition of a second substrate (e.g., glycerol) could stimulate the phenol biodegradation efficiency of strain R186. Hence, a feasible EFS was developed for fed-batch phenol biodegradation using the dual-substrate biostimulation technique. The phenol degradation kinetics was well characterized with proposed model and response surface analysis. Our findings quantitatively revealed that glycerol could effectively enhance the phenol degradation performance, as the highest phenol degradation efficiency occurred with the supplementation of 0.8–1.2 g L^{-1} of glycerol. The optimal dual-substrate EFS was identified via contour analysis and kinetic modeling. With the optimal dual-substrate EFS (i.e., a feeding rate constant (α_1 and α_2) of 0.5 and 0.3, respectively), the shortest time (ca. 13.80 h) for phenol degradation was achieved with a specific growth rate of ca. 0.281 h^{-1}.

1. Introduction

Cupriavidus taiwanensis R186 (former taxonomy of *Cupriavidus* was *Ralstonia*; R186, for short) isolated from southwest Taiwan demonstrated an excellent capability to grow on a medium containing phenol or trichloroethylene (TCE) as a carbon source [1,2]. Compared to other phenol biodegraders [2,3], R186 displayed a superior phenol biodegradation ability as well as high tolerance (up to ca. 900 mg/L) in the phenol-laden media. According to Haldane's model for phenol degradation of *R. taiwanensis* (i.e., *C. taiwanensis*) [2], the optimal degradation rate was 61 μmol/mol/g cell occurring at a phenol concentration of 228 μM. In addition, the low saturation constant (K_S) of 5.46 μM and high inhibition constant of 9075 μM suggested a promising potential of using R186 for practical bioremediation [2]. As indicated in previous studies [4,5], the indigenous rhizobium *C. taiwanensis* R186 was feasible to be used for bioremediation of phenol-contaminated soil, freshwater and wastewater.

As phenol degradation capacity was strongly dependent upon cell population size per unit volume. Thus, achieving a high cell density process may be a key to an efficient phenol biodegradation process [6]. Fed-batch cultures have been successfully used to achieve high cell density and avoid substrate inhibition [6]. Fed-batch culture is advantageous in particular when nutrient concentrations strongly affect cell yield or productivity, as both overfeeding and underfeeding would result in growth repression and starvation to cells, respectively [7]. Thus, to maintain a maximal cell growth within the exponential growth phase, the nutrient feeding should be in a parallel increasing profile to compensate optimal cell needs for the maximal productivity. As a result, our recent work [8] selected fed-batch modes of operation via exponential feeding strategy (EFS) to maximize cell density while using phenol as a sole carbon source for optimal phenol degradation. The optimal feeding strategy for exponential growth was obtained at approximately $\alpha = 0.50–0.55\mu_{max}$ [8]. Moreover, to provide optimal biostimulation strategy for maximization of the performance of phenol degradation, we first considered the approach of toxicity reduction of phenol via cloaking of augmented nutrient source [5]. Our findings indicated that among several augmented carbon sources examined, glycerol appeared to be the best augmented carbon substrate, allowing effective enhancement of phenol degradation with simultaneous utilization of glycerol and phenol for cellular growth, instead of diauxic growth [5]. The phenomenon of non-diauxic consumption of dual substrates seems to make glycerol an ideal biostimulation nutrient supplement to stimulate phenol biodegradation.

Therefore, this study was undertaken to reveal whether the fed-batch mode of operation under exponential feeding strategy of dual substrates (i.e., glycerol and phenol) could be the most efficient bioreactor operation for phenol biodegradation to achieve a min-

* Corresponding author at: Department of Chemical Engineering, National Cheng-Kung University, Tainan 701, Taiwan. Fax: +886 6 2357146.
E-mail address: changjs@mail.ncku.edu.tw (J.-S. Chang).

0304-3894/$ – see front matter © 2009 Elsevier B.V. All rights reserved.
doi:10.1016/j.jhazmat.2009.02.045

Nomenclature

F_{10}	phenol feeding rate (mL min^{-1})
F_{20}	glycerol feeding rate (mL min^{-1})
J	objective function for the squared error sum between experimental data and prediction curve
K_{S_1}	half-saturation coefficient of phenol (g L^{-1})
K_{S_2}	half-saturation coefficient of glycerol (g L^{-1})
K_i	phenol inhibition constant (g L^{-1})
K'	enhancement coefficient of phenol degradation (g L^{-1})
S_1	phenol concentration in the broth (g L^{-1})
S_2	glycerol concentration in the broth (g L^{-1})
S_{10}	phenol concentration in the feed (g L^{-1})
S_{20}	glycerol concentration in the feed (g L^{-1})
$\hat{S}_{1i}$	phenol concentration predicted by kinetics (g L^{-1})
$\hat{S}_{2i}$	glycerol concentration predicted by kinetics (g L^{-1})
S_{1m}	initial phenol concentration (g L^{-1})
S_{2m}	initial glycerol concentration (g L^{-1})
S^*	the substrate concentration at the maximal specific growth rate (g L^{-1})
t	culture time (h)
t_p	predicted time requirement for complete phenol degradation using second-order polynomial (h)
t_k	predicted time requirement for complete phenol degradation according to the kinetic model (h)
$t_f^{\exp}$	experimental total time required for complete phenol degradation (h)
V	working volume (L)
X	cell concentration (g L^{-1})
X_m	maximal cell concentration (g L^{-1})
X_i	cell concentration of ith experimental data point (g L^{-1})
$\hat{X}_i$	predicted cell concentration of ith data point (g L^{-1})
Y_{X/S_1}	yield coefficient of phenol substrate converted to biomass (g cell/g phenol)
Y_{X/S_2}	yield coefficient of glycerol substrate converted to biomass (g cell/g glycerol)
μ_1	specific growth rate due to phenol degradation (h^{-1})
μ_2	specific growth rate due to glycerol consumption (h^{-1})
$\mu_{\max_1}$	maximal specific growth rate based on phenol degradation (h^{-1})
$\mu_{\max_2}$	maximal specific growth rate based on glycerol consumption (h^{-1})
μ'	modified specific growth rate in dual-substrate systems (h^{-1})
α_1	pre-set value of phenol feeding rate constant
α_2	pre-set value of glycerol feeding rate constant

imal time required for removal of a fixed amount of phenol. As known, Pontryagin's maximum principle could be used for determining optimal operation strategy for single-control variable (e.g., temperature, feeding rate); however, such an approach seemed to be not so appropriate to describe multiple-variable systems (e.g., this study) perhaps due to complicated combined interactions between responses and control variables. This is why we carried out this so-called "experimental optimization" for dual-substrate systems. This follow-up study aimed to maximize phenol degradation by toxicity attenuation of phenol via biostimulation of augmented nutrient source. Our recent work has developed the optimal EFS for phenol-only cultures based on kinetic models describing growth patterns and the expected phenol demand. However, the optimal EFS for simultaneous addition of dual substrates has not been explored yet. This study tended to link optimal biostimulation strategy with fed-batch EFS operation [8] of dual substrates to achieve maximal phenol degradation rate as a novel attempt to develop a promising phenol degradation bioprocess. To perform this novel approach, we first provided kinetic modeling upon appropriate operation domains by quantifying combined interactions of glycerol and phenol. Then, the performance index was set as the minimal time required to completely degrade a fixed amount of phenol (i.e., 3.0 g). Next, our kinetic model prediction coupled with response surface analysis showed the most likely optimal ranges of feeding rate constants for each substrate (α_1, α_2). Within this optimal domain, five sets of (α_1, α_2) were selected to determine and confirm the optimal feeding rate constants. The results revealed that our proposed model was appropriate to describe the kinetic behavior and to predict optimal operation conditions for simultaneous exponential feeding of the dual substrates.

2. Materials and methods

2.1. Bacterial strains and culture conditions

C. taiwanensis R186 originally isolated from root nodules of *Mimosa pudica* in southern Taiwan [1,2] was routinely grown at 28 °C on LB broth consisting of (g L^{-1}): tryptone 10, yeast extract 5.0, NaCl 10. For phenol degradation experiments, a single colony grown on LB agar plate was strain R186 was inoculated to 50 mL of phenol-amended (ca. 200 mg L^{-1} in general) basal salt (BS) medium (KH_2PO_4 3.0 g L^{-1}, Na_2HPO_4 7.0 g L^{-1}, NaCl 0.5 g L^{-1}, NH_4Cl 1.0 g L^{-1}; pH 6.8 ± 0.2) for flask cultures incubated at 37 °C with 200 rpm shaking for 24 h. This 24 h culture was then subject to centrifugation (9000 × *g*, 2 min, Hettich Universal 32R, Germany). The cell pallets were harvested and dissolved in 10 mL phosphate buffer saline. The resulting cell slurry was then inoculated into a 5-L fermentor for phenol degradation study (inoculum size, 0.1 g L^{-1}; initial working volume, 1.0 L; agitation rate, 250 rpm; aeration rate, 1 vvm). The medium used in fermentation study contained BS medium, 200 mg L^{-1} phenol and trace metal ions ($FeSO_4{\cdot}7H_2O$, 7.0 mg L^{-1}; $MgSO_4{\cdot}7H_2O$, 580 mg L^{-1}; $CaCl_2$, 59.3 mg L^{-1}; $MnSO_4{\cdot}H_2O$, 0.385 mg L^{-1}; $CoCl_2{\cdot}6H_2O$, 0.20 mg L^{-1}; $CuSO_4{\cdot}5H_2O$, 53.5 μg L^{-1}).

2.2. Analytical assessments

2.2.1. Sample assay

Cell concentration in culture media was monitored by the absorbance at 600 nm (OD_{600}) using UV–vis spectrophotometer (Hitachi U-2001 spectrophotometer, Tokyo, Japan). The concentration of phenol in the medium was determined by using a colorimetric assay with a detection limit of ±2.5 μM as described elsewhere [5]. The colorimetric reagent used for phenol assay contained pH 10 buffer (HBr 3.0 g L^{-1}, KCl 3.73 g L^{-1}, NaOH 1.76 g L^{-1}), 4-aminoantipyrine and potassium hexacyanoferrate.

2.2.2. Phenol degradation characteristics

The specific growth rate (μ) and specific phenol degradation rate (q_p) were determined through the relationships of $(1/X)(dX/dt)$ and $(-1/X)(d[PhOH]/dt)$, respectively; where X, $[PhOH]$, and t denote cell concentration, phenol concentration, and incubation time, respectively [9,10].

2.2.3. Glycerol analysis

After centrifugation, the supernatant was filtered by 0.2 μm filter to guarantee complete removal of residual solid impurities. The content of glycerol was determined by HPLC (Shimadzu,

Model LC-10AT, Tokyo, Japan) using refraction index detector (Shimadzu RID-10A). The column used for HPLC analysis was ICSep ICE-COREGEL 87H3 column obtained from Transgenomic Inc. (USA).

2.3. Design of exponential feeding strategy

For fed-batch cultures, strain R186 was inoculated into a 5-L fermentor containing 1.0 L of phenol-amended BS medium (phenol concentration = 200 mg L^{-1}). The fermentor was operated at 37 °C, 200 rpm agitation, and pH 7.0 with an aeration rate of 1 vvm. According to Chen et al. [8], the culture was initially operated on batch mode. When 200 mg L^{-1} phenol in the batch system was completely degraded (a dissolved oxygen (DO) spike appeared rapidly), the feeding of dual substrates was conducted immediately. The total amount of dual substrate-bearing solution fed into the fermentor during the fed-batch phenol degradation experiments was 2 L of phenol (S_1) at an inlet concentration of 1500 mg L^{-1} (i.e., 3.0 g of phenol in total) and 1 L of glycerol (S_2) at an inlet concentration of 5000 mg L^{-1} (i.e., 5.0 g of glycerol in total). Based upon model formulation of feeding rates, we could determine feeding rates as a function of time (Appendices A and B). Once the feeding rates were too large to result in phenol accumulation (i.e., $dS_1/dt > 0$), the exponential feeding of both substrates was switched to constant-rate feeding. Our performance index was to minimize the time required to degrade the designated amount (3.0 g) of phenol. For comparison on the same basis with the results indicated in Chen et al. [8], we specifically selected the "batch-and-then-fed-batch" mode of operation in this study. That is, the system is operated at batch mode ($F = 0$) for bang–bang control and then in fed-batch mode ($F(t)$ = singular feeding, such as exponential feeding profile(s)) for singular control as indicated in Chen et al. [8] and Pontryagin's maximum principle [11]. Then, comparative analysis upon the effects of EFS for dual substrates was provided to determine optimal set of feeding rate constants (i.e., α_1 and α_2). According to Appendix B, the feeding rate of phenol (F_{10}) and glycerol (F_{20}) is shown as follows (Eqs. (B.9) and (B.10)):

$$F_{10} = \frac{\mu_1 e^{S_2/K'} V_0 X_0 e^{\mu' t}}{Y_{X/S_1}(S_{10} - S_1)} + \frac{F_{20} S_1}{(S_{10} - S_1)} \approx \frac{\mu_1 e^{S_2/K'} V_0 X_0 e^{\mu' t}}{Y_{X/S_1} S_{10}},$$

$$F_{20} = \frac{\mu_2 V_0 X_0 e^{\mu' t}}{Y_{X/S_2}(S_{20} - S_2)} + \frac{F_{10} S_2}{(S_{20} - S_2)},$$

where $\mu' = \mu_1 + \mu_2 = \alpha_1 \mu_{\max_1} + \alpha_2 \mu_{\max_2}$. The feeding equations shown here would be different from those determined via the typical high cell density fed-batch fermentation due to dilution effects of low substrate concentration bearing inlet streams.

3. Results and discussion

3.1. Identification of kinetic model for single-substrate system

Previous studies [5,8] indicated that the Haldane model $\mu_1 = \mu_{\max_1} S_1/(K_{S1} + S_1 + (S_1^2/K_i))$ could appropriately describe the cell growth profile in phenol-bearing cultures as phenol was inhibitory to cell growth. The maximum specific growth rate $\mu_1^* = \mu_{\max_1}/(1 + 2\sqrt{K_{S_1}/K_i})$ took place at a phenol concentration $S_1^* = \sqrt{K_{S_1} K_i}$. At low phenol concentration (i.e., negligible phenol inhibition), the maximal specific growth rate $\mu_{\max_1}$ and half-saturation coefficient K_{S_1} could simply be obtained via Lineweaver–Burk plot. Next, from the plot of specific growth rate versus phenol concentration, one could find the concentration (S_1^*) corresponding to the maximum specific growth rate. The inhibition constant K_i could then be estimated by $S_1^* = \sqrt{K_{S_1} K_i}$. The overall yield coefficient Y_{X/S_1} can be evaluated by the ratio of produced cell concentration to consumed substrate concentration ($-\Delta X/\Delta S$). According to this calculation

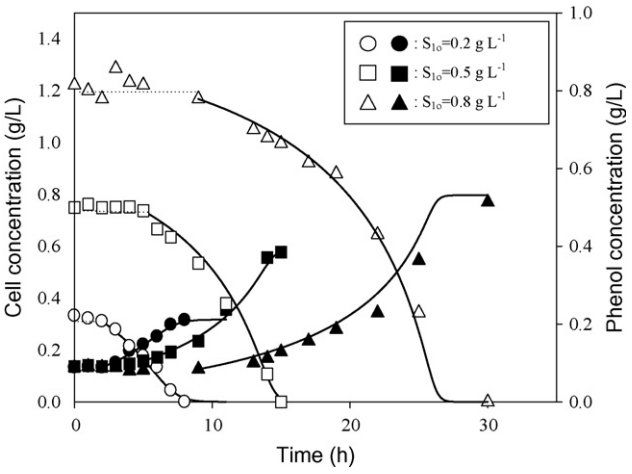

Fig. 1. Kinetic simulation of phenol degradation (open symbols) and cell growth (closed symbols) of *C. taiwanensis* in batch cultures at different initial phenol concentration (S_{10}). The curves indicate the simulation results, while symbols represent the experimental data.

scheme, the values of the kinetic parameters were obtained from simulation of Fig. 1 as $\mu_{\max_1} = 0.50\ h^{-1}$, $K_{S_1} = 0.061\ g\,L^{-1}$, $K_i = 0.28\ g\,L^{-1}$ and $Y_{x/s_1} = 0.908$ g cell/g phenol. To guarantee the stable convergence of calculations for parameter estimation, we used Runge–Kutta method and recursive formulation (Appendix A) to obtain time courses of cell and phenol concentration by setting a convergence scheme of half-step size (i.e., $\Delta t = 0.1$ h and $\Delta t = \Delta t/2 = 0.05$ h; [12]) until $(||(df|_{\Delta t} - df|_{\Delta t/2})||/||df|_{\Delta t/2}||) < 0.05$ was achieved as criteria of iterations, where df denoted state variable X, S_1 or S_2. Following this protocol, we obtained predicted time courses of cell and phenol concentrations which were well-fitted to the experimental results (e.g., $S_{10} = 0.2$–$0.8\ g\,L^{-1}$; Fig. 1).

Compared to phenol, glycerol seemed not to express inhibitory characteristics to *C. taiwanensis* (i.e., $K_i \to \infty$) in Haldane model. Thus, the kinetics of cell growth in glycerol-bearing cultures followed the Monod kinetics: $\mu_2 = \mu_{\max_2} S_2/(K_{S_2} + S_2)$. As described previously, the values of the kinetic parameter could be attained obtained from simulation of Fig. 2 as $\mu_{\max_2} = 0.058\ h^{-1}$, $K_{S_2} = 0.53\ g\,L^{-1}$ and $Y_{X/S_2} = 0.15$ g cell/g glycerol. With these estimated parameters for kinetic simulation, we also obtained well-fitted results between model prediction and experimental data (Fig. 2).

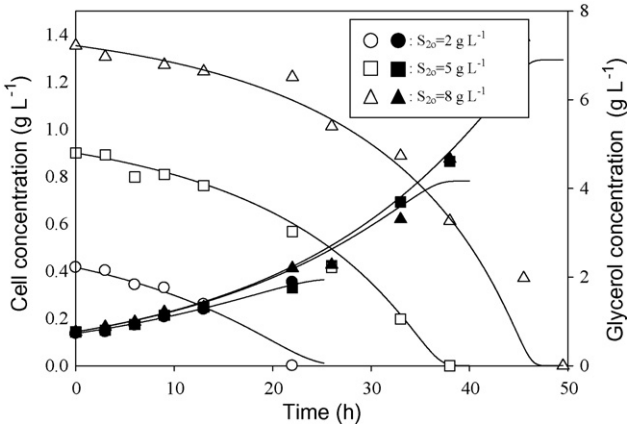

Fig. 2. Kinetic simulation of glycerol utilization (open symbols) and cell growth (closed symbols) of *C. taiwanensis* in batch cultures using glycerol as the sole carbon source. S_{20} denotes initial glycerol concentration. The curves indicate the simulation results, while symbols represent the experimental data.

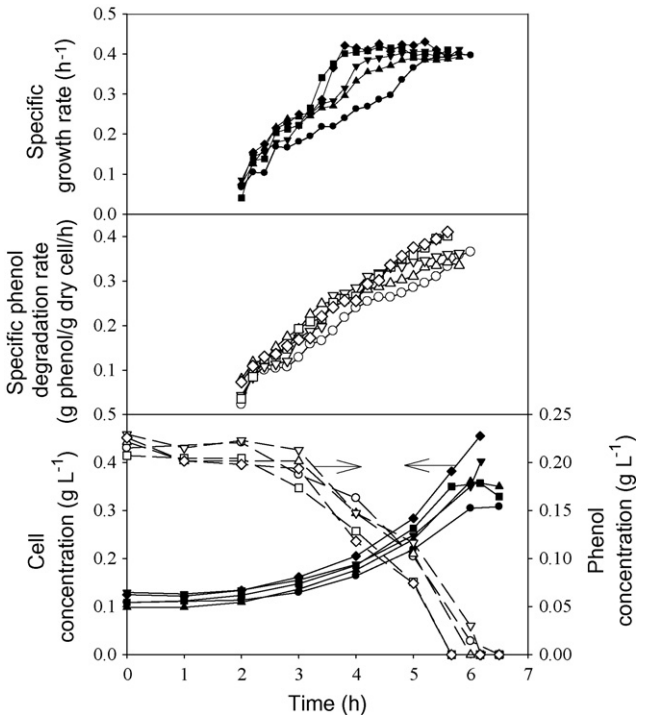

Fig. 3. Time courses of phenol degradation and cell growth using dual substrates and specific growth rate (solid symbol) and phenol degradation rate (open symbol) in batch cultures initially contained 0.2 g L^{-1} phenol combined with glycerol in different concentrations. Phenol 0.2 g L^{-1} alone (●, ○), augmented glycerol 0.2 g L^{-1} (▲, △), 0.4 g L^{-1} (▼, ▽), 0.6 g L^{-1} (■, □), 0.8 g L^{-1} (♦, ◊).

3.2. Effects of augmented glycerol on phenol degradation

As this study tended to use dual substrates as a biostimulation strategy for efficient phenol degradation and optimal growth of R186, the effects of combined interactions between glycerol and phenol were inspected. To reveal the enhancement effect on phenol degradation arising from biostimulation with glycerol addition, we conducted batch experiments for degradation of 0.2 g L^{-1} phenol in the presence of glycerol at 0.2–0.8 g L^{-1}. As seen in Fig. 3, 3 h lag phases were all observed at 0.2 g L^{-1} phenol alone and in the presence of glycerol tests. However, due to glycerol enhancement, phenol degradation was approximately completed at ca. 6 h, which is shorter than that obtained from using 0.2 g L^{-1} phenol alone. In particular, for addition of 0.6 and 0.8 g L^{-1} glycerol, the time required for complete phenol degradation was further shortened to ca. 5.5 h. This shows that glycerol could enhance the efficiency of phenol degradation.

To quantitatively clarify this biostimulation effect, we also determined specific growth and specific phenol degradation rate over time for comparison [10]. As shown in Fig. 3, the specific growth rate progressively increased in the exponential growth phase. Cultures bearing with glycerol 0.6 and 0.8 g L^{-1} showed higher specific growth rates than the others (e.g., the lowest for the case of phenol alone). Apparently, the augmentation of glycerol could effectively enhance/stimulate phenol degradation in the exponential growth phase (Fig. 3). This again confirms that glycerol could stimulate phenol degradation as proposed in our recent work [5].

3.3. Fractional food to microorganism (F:M) ratio

To uncover the combined interactions among lag time, phenol degradation time and specific growth rate, we introduced a fractional "food to microorganism (F:M) ratio" for the quantitative evaluation upon glycerol enhancement to phenol degradation

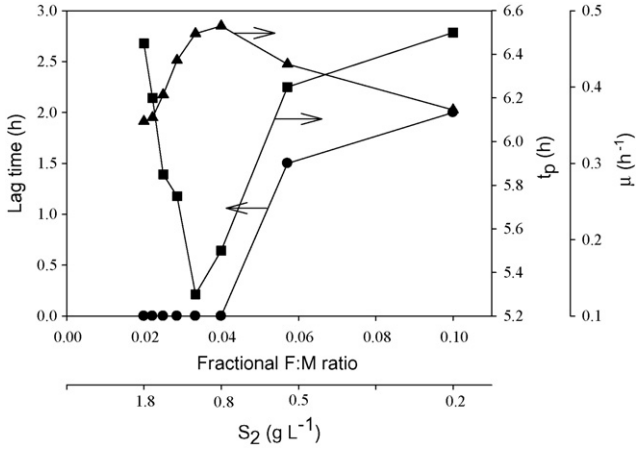

Fig. 4. The effects of augmented glycerol (S_2) and fractional F:M ratio on lag time (●), time required for complete phenol degradation (t_p) (■) and specific growth rate (μ) (▲).

[13]. The F:M ratio was defined herein as the phenol substrate load applied to the process per unit of biomass in cultures. For dual-substrate systems, this term was re-defined as the measure of fractional F:M ratio (i.e., $(S_1/X_0)(S_1/(S_1+S_2))$), indicating the apparent contribution of phenol substrate in dual substrates per unit biomass. That is, an increase in glycerol concentration would result in a reduction in phenol toxicity since $S_1/(S_1+S_2)<1$ or $(S_1/X_0)(S_1/(S_1+S_2))<S_1/X_0$. In contrast, if glycerol was added in a trace amount (e.g., $S_1/(S_1+S_2)\rightarrow 1$), the effect of glycerol enhancement would be negligible (or $(S_1/X_0)(S_1/(S_1+S_2))\fallingdotseq S_1/X_0$). However, when glycerol is supplemented in a sufficiently high level (i.e., $S_1/(S_1+S_2)\rightarrow 0$), phenol toxicity no longer exists, as cells would seemingly grow on the predominant substrate (i.e., glycerol) alone (e.g., $S_2>1.2$ g L^{-1}; Fig. 4). Thus, the appropriate glycerol concentration for optimal enhancement would fall in a certain range (i.e., 0.8–1.2 g L^{-1}; Fig. 4). In addition, as $S_2 \ll S_1$, phenol toxicity would be maximized and thus phenol degradation would be significantly decreased (e.g., $S_2<1.2$ g L^{-1}; Fig. 4). As revealed in Fig. 4, the lag time was still be long at high-level fractional F:M ratios due to phenol inhibition/toxicity (i.e., S_1 was sufficiently large). When the fractional F:M ratio was relatively low, apparently the time for phenol degradation (t_p) also increased due to preferable utilization of glycerol (e.g., relatively low phenol to glycerol ratio). Thus, the shortest time for phenol degradation and lag time was approximately at glycerol concentration of ca. 0.8–1.2 g L^{-1} (i.e., a fractional F:M ratio of 0.04; Fig. 4). Excessive glycerol addition seemed to delay the time required for phenol degradation as glycerol would mask the presence of phenol. Therefore, maintaining glycerol concentration at the optimal range (i.e., ca. 0.8–1.2 g L^{-1}) could provide the most effective phenol degradation in the fed-batch cultures.

3.4. Reconstruction of kinetic model for dual-substrate system

Since the augmentation of glycerol apparently enhanced cell growth as well as phenol degradation, it was crucial to propose a kinetic model for cultures involving the dual-substrate phenol degradation system. To uncover the effects of glycerol enhancement to cell growth [5], a modified term ($e^{S_2/K'}$) was introduced to describe the enhancing effect of glycerol (S_2) on growth kinetics according to phenol consumption (Eq. (1)). K' is an empirical parameter representing the power of biostimulation effect of glycerol. The presence of this modified term strongly supports that synergistic interactions of glycerol significantly affect the performance of phenol degradation. This parameter should satisfy asymptotic behaviors to include all properties in phenol-alone systems (i.e.,

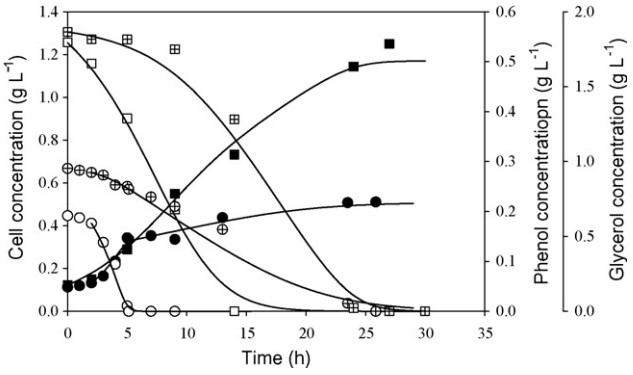

Fig. 5. Kinetic simulation of batch cultures using dual substrates of glycerol and phenol at high (squares) and low (circles) initial concentrations (○, □: phenol concentration; ⊕, ⊞: glycerol concentration; ●, ■: cell concentration).

$S_2 \to 0$) as follows:

$$\lim_{S_2 \to 0} \frac{\mu_{\max_1} S_1}{K_1 + S_1 + S_1^2/K_i} e^{S_2/K'} = \frac{\mu_{\max_1} S_1}{K_1 + S_1 + S_1^2/K_i}. \quad (1)$$

Aware that the introduced parameter K' denoted a biostimulation power of glycerol to cell growth. Apparently, this parameter must satisfy certain basic properties as follows:

1. $\lim_{K' \to \infty} e^{S_2/K'} = 1$,
2. $+\infty = \lim_{K' \to 0} e^{S_2/K'} > e^{S_2/K'}|_{0<K'<+\infty} > \lim_{K' \to \infty} e^{S_2/K'} = 1$.

Criterion 1 indicates that a complete inhibition of augmented substrate to cell growth would take place at $K' \to \infty$. Criterion 2 suggests that a decrease in the parameter K' could increase this enhancement power for biostimulation. Then, we could obtain the overall specific growth rate as follows:

$$\mu = \mu_1 + \mu_2 = \frac{\mu_{\max_1} S_1}{K_1 + S_1 + (S_1^2/K_i)} e^{S_2/K'} + \frac{\mu_{\max_2} S_2}{K_2 + S_2}. \quad (2)$$

With given parameter values, we could obtain time courses of state variables (X, S_1, S_2) via solving state equations (Appendices A and B). To estimate the optimal parameter K' for a best fit, the objective function J was then defined as the sum of squared error as follows:

$$J = \sum_{i=1}^{n} \left\{ \frac{1}{X_m^2}(X_i - \hat{X}_i)^2 + \frac{1}{S_{1m}^2}(S_{1i} - \hat{S}_{1i})^2 + \frac{1}{S_{2m}^2}(S_{2i} - \hat{S}_{2i})^2 \right\}, \quad (3)$$

where X_m, S_{1m}, and S_{2m} denoted maximal cell concentration, initial phenol, and glycerol concentration, respectively. To obtain the optimal K' value to minimize the sum of squared errors (i.e., $J_{\min}$), parameter estimation via a random searching technique was carried out. The best-fit value of this empirical parameter K' was obtained as 15.4 g L^{-1}. With this estimated parameter, the model simulation almost provided best prediction for dual-substrate systems (Fig. 5). This kinetic model was adopted to predict feasible exponential feeding profiles for dual substrates in fed-batch systems (Appendix B).

3.5. Set-up of dual-substrate exponential feeding strategy

Our previous findings [8] have identified the optimal exponential feeding strategy for phenol degradation in single-substrate system by using strain R186. The results showed that 3.0 g (2 L × 1.5 g L^{-1}) of phenol was degraded in 15 h including the 6 h for batch growth and 9 h for exponential feeding. In addition, we also found that dissolved oxygen concentration should be less than

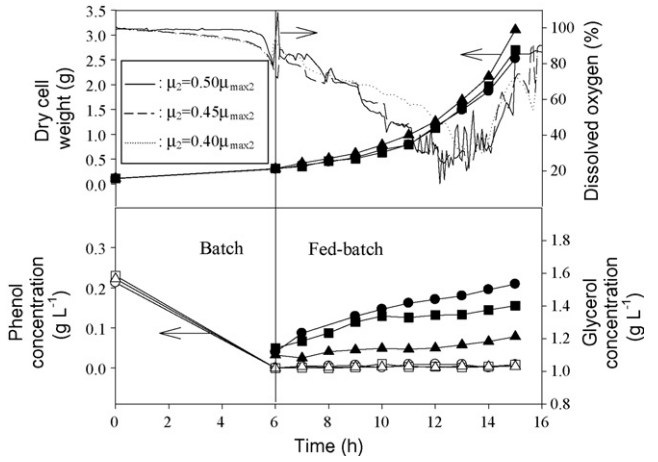

Fig. 6. Accumulation of phenol and glycerol concentration during feeding dual substrate under different α_2 value (●, ○: $\alpha_2 = 0.5$, ■, □: $\alpha_2 = 0.45$, ▲, △: $\alpha_2 = 0.4$). The EFS for phenol substrate was set at $\mu_1 = 0.45\mu_{\max_1}$ and $\mu_2 = \alpha_2\mu_{\max_2}$.

55% to achieve the optimal efficiency of volumetric rate for phenol degradation, while low DO levels caused oxygen-transfer limitation to cell growth. For EFS operation, the optimal DO range was set between 10 and 55% for fed-batch cultures [8]. The foregoing information was utilized to develop the EFS for dual-substrate fed-batch operation when both phenol and glycerol were fed simultaneously at the designated volumetric loading rate.

The most critical parameters to be determined are the exponential feeding rate. For phenol-alone systems, the optimal set point of the specific growth rate of exponential feeding was approximately $0.45\mu_{\max}$–$0.50\mu_{\max}$, that is the feeding rate constant of phenol (α_1) was 0.45–0.50 [8]. For dual-substrate system, glycerol feeding rate becomes an additional criterion, as it should be set at appropriate ranges for optimal operation to avoid overloading or under dosage of glycerol, both resulting in poor biostimulation effect. For a preliminary test on dual-substrate EFS operation, the specific growth rate of phenol feeding was pre-set at $0.45\mu_{\max_1}$ (i.e., $\alpha_1 = 0.45$), while various glycerol exponential feeding rate constants ($\alpha_2 = 0.40$–0.50; Fig. 6) were used under a fixed phenol feeding rate (i.e., $\mu_1 = 0.45\mu_{\max_1}$) (Appendix B). The results show that when $\mu_2 > 0.40\mu_{\max_2}$ progressively increases in residual glycerol concentration were observed after EFS was conducted (Fig. 6). Hence, from the results this preliminary EFS tests, the specific growth rate of glycerol should be set below $0.4\mu_{\max_2}$ to avoid accumulation of glycerol. Apparently, more appropriate feeding rate constants (α_1 and α_2) should be determined to achieve optimal EFS operation, which will be done in the following section.

3.6. Optimization of dual-substrate EFS

With the aid of kinetic modeling (Appendix A) of cultures in dual-substrate systems, we could determine the time required for complete degradation of 3.0 g phenol (t_p) in various sets of rate constants (α_1, α_2), where pre-set values of α_1, α_2 might be obtained as described elsewhere [4,5,8]. We selected collocation points which were well-distributed in the operation domain (i.e., $0.3 < \alpha_1 < 0.55$ and $0.25 < \alpha_2 < 0.4$, which is the region without substrate limitation and inhibition) for model simulation. The responses were reflected onto 2D contour level curves in the coordinate system (x, y-axes in variables α_1, α_2, z-contour (t_p) denoted time required for complete degradation of 3.0 g phenol) predicted from the polynomial model (Eqs. (4) and (5)). Note that the introduction of contour analysis was to eliminate the possible experimental deviations likely due to confounding variances in parameter estimation as indicated in Section 3.4. We could then obtain algebraically in terms of the general

second-order polynomial model as follows:

$$f(\alpha_1, \alpha_2) = \sum_{i=0}^{2}\sum_{j=0}^{2} b_{ij}\alpha_1^i\alpha_2^j. \quad (4)$$

The response contours of time required t_p could be evaluated as follows:

$$t_p = 56.80 - 151.41\alpha_1 - 31.06\alpha_2 + 137.11\alpha_1^2 + 46.54\alpha_1\alpha_2 + 13.38\alpha_2^2. \quad (5)$$

Here, we defined the deviation of the evaluated results as follows:

$$\text{deviation}(\%) = \frac{t_p - t_k}{t_p} \times 100, \quad (6)$$

where t_k denoted the kinetic model-predicted time required for complete phenol degradation (i.e., the time to achieve zero phenol accumulation). Compared with the time required between polynomial model (t_p) and kinetic model (t_k), the deviations were reasonably negligible (all less than 5%; data not shown).

This relatively simple model (i.e., contour-profiles Eq. (5)) instead of the kinetic models could be popularly used by on-site industrial professionals to determine threshold criteria and optimal conditions for operation. To determine the optimal condition of (α_1, α_2) for minimal time t_p, we constructed the level contours according to the response surfaces (Eq. (5) and Fig. 7). We then conducted experimental verification to confirm the practicality and consistency of our proposed level contours (i.e., five data points in Fig. 7). Five selected sets of experiments (α_1, α_2) = (0.50, 0.40), (0.50, 0.35), (0.50, 0.30), (0.48, 0.37), (0.52, 0.32) located within the possible region of optimality were carried out. These sets were chosen due to the shorter time required of phenol degradation than other domains in the predicted contour diagram. With this "experimental optimization", we found that the optimal point was taking place at (α_1, α_2) of around (0.50, 0.30). This optimal feeding strategy (i.e., (α_1, α_2) = (0.50, 0.30)) resulted in the shortest time required for complete phenol degradation (t_p = 13.80 h at overall specific growth rate of 0.281 h^{-1}) (Fig. 7). This 13.80 h (or 7.80 h in fed-batch mode) from our dual-substrate EFS is markedly shorter than that obtained from the EFS for phenol-alone system (15.0 h or ca. 9.12 h in fed-batch mode) [8], indicating that the feasibility of using the approach proposed in this work.

Furthermore, the deviations of response prediction and experimental results of the five points shown in level contours were all less than 5% (Fig. 7), indicating a promising feasibility to adopt level contours in place of kinetic modeling for practical use. In particular, Fig. 8a also shows the details of kinetic simulation and experimental verification for optimal fed-batch cultures via dual-substrate EFS, supporting a promising consistency for our approach. Besides, all other four sets of experimental outcomes also revealed this consistency (data not shown). In addition, the results indicated in Fig. 8a supported that nearly zero phenol accumulation and glycerol at 0.8–1.2 g L^{-1} were indeed the operation criteria for optimality. However, in the fed-batch culture with (α_1, α_2) = (0.50, 0.40), model predication deviated slightly from experimental data due to some residual glycerol concentration relatively larger than the optimal value for biostimulation (ca. 0.8–1.2 g L^{-1}) staring at ca. 11th hour of culture time (Fig. 8b).

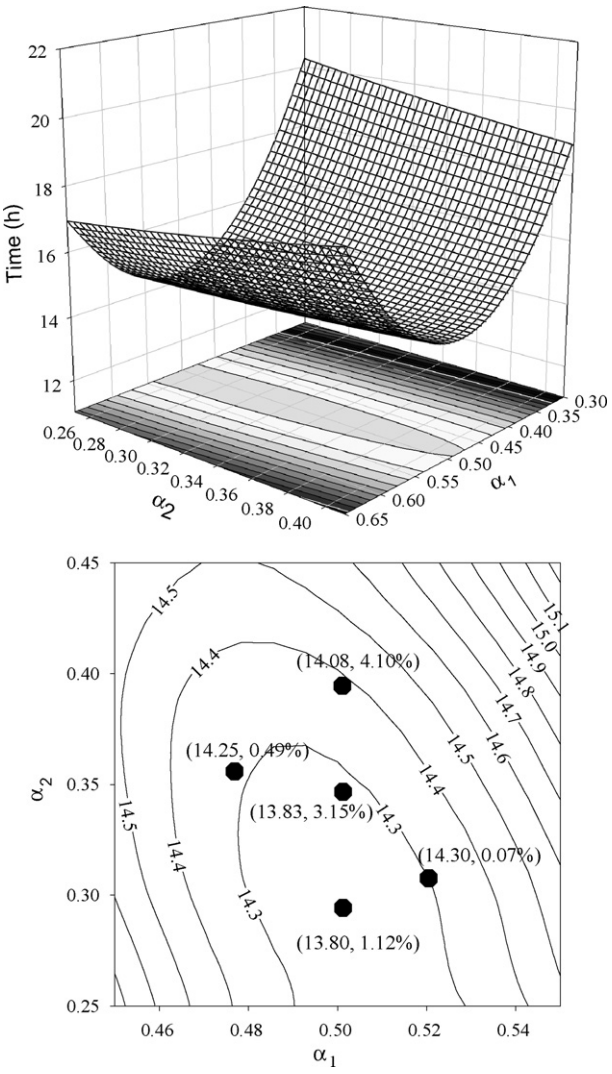

Fig. 7. Prediction surface graph and contour diagram of time required for complete phenol degradation of 3.0 g phenol (1.5 g L^{-1} × 2.0 L). Notation of (x, y) denotes "x" hours required for complete phenol degradation with a deviation of "y" (%) between experimental time and contour prediction.

3.7. Remarks and suggestions

The experimental deviations present in the study were very likely due to some inevitable biochemical characteristics. For example, fed-batch cultures were essentially operated in transient dynamics and the postulates of time-invariant kinetic parameters might only be valid on certain ranges of operation. Thus, it is not so simple to anticipate, in the form(s) of biochemical models, the combined interactions between input variables and output responses. In particular, previous studies [8] could only uncover kinetic characteristics of single-substrate systems. Apparently, complicated interactions would appreciably interfere with kinetic parameters of dual-substrate systems when single-substrate data were used. That was very likely why there was still some experimental deviation even we tended to apply kinetic model to show characteristics of this dual-substrate systems. Moreover, although diauxic growth behavior was not clearly seen in this glycerol–phenol system, metabolic pathways utilizing these two substrates would be somehow different from each other. That is why some modified term was introduced to kinetic modeling for better prediction of time courses of state variables. Apparently, the method as stated herein might be over-simplified to be used as practical values. This point is suspected to be the major cause leading to experimental deviations. To achieve better model predictions, the mysteries of these existing interactions should be disclosed via detailed metabolism studies from the aspect of biochemistry and molecular biology (e.g., structured models or single cell model).

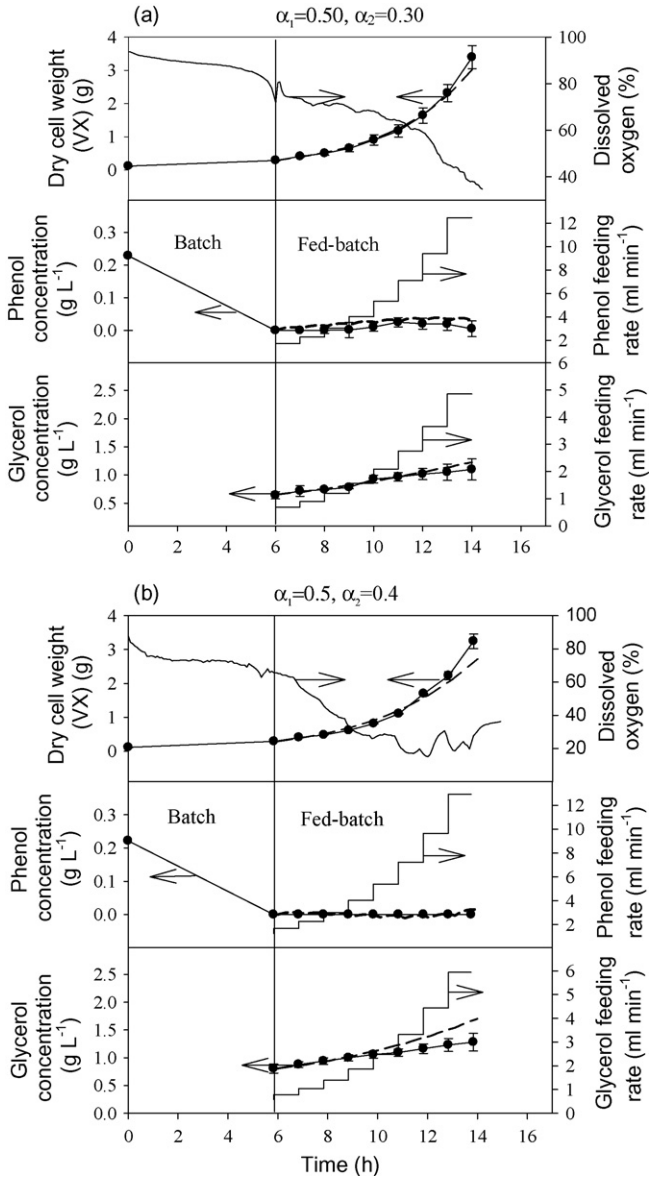

Fig. 8. (a) Time courses of output variables (cell, DO, substrate concentrations and feeding rates in dual-substrate fed-batch culture ($\alpha_1 = 0.50$, $\alpha_2 = 0.30$) for phenol degradation. (b) Time courses of output variables (cell, DO, substrate concentrations and feeding rates in dual-substrate fed-batch culture ($\alpha_1 = 0.50, \alpha_2 = 0.40$) for phenol degradation.

4. Conclusion

This first-attempt study provided the plausible kinetic modeling and response surface analysis to accurately uncover the microbial characteristics of fed-batch system with dual substrates for phenol degradation. It was revealed that glycerol could not only be used as a carbon source for R186, but also effectively enhanced the efficiency of phenol degradation. When the most appropriate amount of glycerol (0.8–1.2 g L^{-1}) was provided in the presence of phenol, R186 could degrade phenol at the highest rates. According to contour analysis and kinetic modeling, the optimal exponential feeding strategy for dual-substrate systems was identified. At the optimal EFS at $(\alpha_1, \alpha_2) = (0.5, 0.3)$ for dual substrates of the fed-batch culture, the shortest time for phenol degradation (ca. 13.80 h) was obtained and its specific growth rate was ca. 0.281 h^{-1}.

Acknowledgements

Financial supports (NSC 95-2221-E-197-005, NSC 96-2221-E-197-012, NSC 97-2221-E-197-019) from National Science Council, Taiwan, ROC. for this research are very much appreciated. The authors also extend sincere appreciation to anonymous reviewers for significant comments and valuable suggestions.

Appendix A. Model prediction of cell growth and substrate consumption

A.1. Fed-batch culture

To present time courses of cell growth and substrate consumption, we formulate the mass balances on biomass and substrate as shown below:

$$\frac{d(VX)}{dt} = V\frac{dX}{dt} + X\frac{dV}{dt} = \mu' VX, \tag{A.1}$$

$$\frac{d(VS_i)}{dt} = F_{i0}S_{i0} - \frac{\mu_i VX}{Y_{X/S_i}} \quad \forall i = 1,\ 2. \tag{A.2}$$

A.2. Biomass balance

The mass balance of biomass could be obtained as follows:

$$V\frac{dX}{dt} + X\frac{dV}{dt} = \mu' VX. \tag{A.3}$$

If total control volume $dV/dt = \sum_i F_i$ was introduced, the biomass balance could thus be reformulated as follows:

$$V\frac{dX}{dt} = \mu' VX - X\frac{dV}{dt} = X\left(\mu' V - \sum_i F_i\right). \tag{A.4}$$

Thus, the discrete formulation of cell concentration at various times could be obtained as

$$X_{i+1} = X_i + \left(\mu' - \frac{\sum_i F_i}{V}\right) X_i \Delta t. \tag{A.5}$$

A.3. Dual-substrate balance

In addition, time-dependent substrate concentration could be resulted according to mass balance on substrates as follows ($\forall i = 1, 2$):

$$\frac{d(VS_i)}{dt} = S_i\frac{dV}{dt} + V\frac{dS_i}{dt} = F_{i0}S_{i0} - \frac{\mu_i VX}{Y_{X/S_i}}. \tag{A.6}$$

We then reformulated these state equations on S_1, S_2 as follows:

$$V\frac{dS_i}{dt} = F_{i0}S_{i0} - S_i\frac{dV}{dt} - \frac{\mu_i VX}{Y_{X/S_i}}, \tag{A.7}$$

$$\frac{dS_i}{dt} = \frac{F_{i0}}{V}S_{i0} - \frac{S_i}{V}\left(\sum_i F_i\right) - \frac{\mu_i X}{Y_{X/S_i}}. \tag{A.8}$$

That is, the discrete formulation of dual substrates could thus be resulted as follows:

$$S_{i+1} = S_i + \left(\frac{F_{i0}}{V}S_{i0} - \frac{S_i}{V}\left(\sum_i F_i\right) - \frac{\mu_i X}{Y_{X/S_i}}\right)\Delta t. \tag{A.9}$$

If all estimated kinetic parameters were provided, one might obtain the predicted time courses of all state variables by solving simultaneous discrete equations.

Appendix B. Determination of dual-substrate feeding strategy

If lag phase in the growth curve was excluded, we could formulate state equations for cell concentration (X), substrate concentrations (S_1, S_2) in the culture system with the assumption of time-invariant specific growth rate μ' (i.e., exponential growth phase) as follows:

$$VX = V_0X_0e^{\mu' t}. \tag{B.1}$$

As glycerol enhances phenol degradation [5], the specific growth rate μ' in dual-substrate systems could be modified by the following rate expression:

$$\mu' = \mu_1 e^{S_2/K'} + \mu_2. \tag{B.2}$$

Note that for single phenol substrate the asymptotic behavior must satisfy as $\lim_{S_2\to 0}\mu' = \lim_{S_2\to 0}(\mu_1 e^{S_2/K'} + \mu_2) = \mu_1$. Regarding mass balance on two substrates S_1, S_2, phenol and glycerol consumption can be termed as follows:

$$\frac{d(VS_1)}{dt} = F_{10}S_{10} - \frac{\mu_1 e^{S_2/K'}(VX)}{Y_{X/S_1}}, \tag{B.3}$$

$$\frac{d(VS_2)}{dt} = F_{20}S_{20} - \frac{\mu_2(VX)}{Y_{X/S_2}}. \tag{B.4}$$

In addition, to avoid phenol accumulation to result in poor cellular activity for phenol degradation, the technique of DO spike was used as a probing indicator to reveal the time of exhaustion of phenol and glycerol. Then, a basic strategy of feed-forward control to adjust exponential feeding was resulted. Considering mass balances on two substrates, we may formulate as follows:

$$\frac{d(VS_i)}{dt} = V\left(\frac{dS_i}{dt}\right) + S_i\left(\frac{dV}{dt}\right) \quad \forall i = 1,\ 2. \tag{B.5}$$

If the residual substrate concentration should remain to be approximately fixed (i.e., minimal inhibitory and maximal growth effects) during the feeding phase, we may set up constraint conditions as follows:

$$\left(\frac{dS_i}{dt}\right) \cong 0, \tag{B.6}$$

$$\left(\frac{dV}{dt}\right) = F_{10} + F_{20}. \tag{B.7}$$

In the exponential growth phase, the expression (B.3) could be modified to be

$$V\frac{dS_1}{dt} + S_1\frac{dV}{dt} = F_{10}S_{10} - \frac{\mu_1 e^{S_2/K'}VX}{Y_{X/S_1}}. \tag{B.3′}$$

Substituting Eqs. (B.6) and (B.7) into (B.3′), we could obtain the following relationship:

$$S_1(F_{10} + F_{20}) = F_{10}S_{10} - \frac{\mu_1 e^{S_2/K'}VX}{Y_{X/S_1}}. \tag{B.8}$$

(B.8) can be further reformulated as

$$F_{10} = \frac{\mu_1 e^{S_2/K'}V_0X_0e^{\mu' t}}{Y_{X/S_1}(S_{10} - S_1)} + \frac{F_{20}S_1}{(S_{10} - S_1)} \approx \frac{\mu_1 e^{S_2/K'}V_0X_0e^{\mu' t}}{Y_{X/S_1}S_{10}}. \tag{B.9}$$

Similarly, the feeding strategy for second substrate can be obtained as follows:

$$F_{20} = \frac{\mu_2 V_0X_0e^{\mu' t}}{Y_{X/S_2}(S_{20} - S_2)} + \frac{F_{10}S_2}{(S_{20} - S_2)}, \tag{B.10}$$

where $\mu' = \mu_1 + \mu_2 = \alpha_1\mu_{\max_1} + \alpha_2\mu_{\max_2}$.

References

[1] W.M. Chen, S. Laevens, T.M. Lee, T. Coenye, P. de Vos, M. Mergeay, P. Vandamme, *Ralstonia taiwanensis* sp nov., isolated from root nodules of *Mimosa* species and sputum of a cystic fibrosis patient, Int. J. Syst. Evol. Microbiol. 51 (2001) 1729–1735.

[2] W.M. Chen, J.S. Chang, C.H. Wu, S.C. Chang, Characterization of phenol and trichloroethene degradation by the rhizobium *Ralstonia taiwanensis*, Res. Microbiol. 155 (2004) 672–680.

[3] B.R. Folsom, P.J. Chapman, P.H. Pritchard, Phenol and trichloroethylene degradation by *Pseudomonas cepacia* G4: kinetics and interactions between substrates, Appl. Environ. Microbiol. 56 (1990) 1279–1285.

[4] B.Y. Chen, J.S. Chang, Phenol degradation and toxicity assessment upon biostimulation to an indigenous rhizobium *Ralstonia taiwanensis*, Biotechnol. Prog. 21 (2005) 1085–1092.

[5] B.Y. Chen, W.M. Chen, J.S. Chang, Optimal biostimulation strategy for phenol degradation with indigenous rhizobium *Ralstonia taiwanensis*, J. Hazard. Mater. 139 (2007) 232–237.

[6] L. Yee, H.W. Blanch, Recombinant protein expression in high cell density fed-batch cultures of *Escherichia coli*, Biotechnology 10 (1992) 1550–1556.

[7] A.S.M. Miguel, M. Vitolo, A. Pessoa Jr., Fed-batch culture of recombinant *Saccharomyces cerevisiae* for glucose 6-phosphate dehydrogenase production, Biochem. Eng. J. 33 (2007) 248–252.

[8] B.Y. Chen, J.W. You, Y.T. Hsieh, J.S. Chang, Feasibility study of exponential feeding strategy in fed-batch cultures for phenol degradation using *Cupriavidus taiwanensis*, Biochem. Eng. J. 41 (2008) 175–180.

[9] J.E. Bailey, D.F. Ollis, Biochemical Engineering Fundamentals, 2nd ed., McGraw-Hill Inc., New York, 1986.

[10] B.Y. Chen, Understanding decolorization characteristics of reactive azo dye by *Pseudomonas luetola*: toxicity and kinetics, Proc. Biochem. 38 (2002) 437–446.

[11] D.E. Kirk, Optimal Control Theory: An Introduction, Prentice Hall, 1970.

[12] B.Y. Chen, Biologically-feasible screening strategy for optimal decolorization strain to diazo Evercion Red H-E7B, J. Chin. Inst. Chem. Eng. 37 (2006) 117–124.

[13] L.D. Benefield, C.W. Randall, Biological Process Design for Wastewater Treatment, 1st ed., Prentice-Hall Inc., New York, 1980.